Naval Research Laboratory

Washington, DC 20375-5320

AD-A257 983

Identification of Toroidal Field Errors
In a Modified Betatron Accelerator

P. LOSCHIALPO AND C.A. KAPETANAKOS

Beam Physics Branch
Plasma Physics Division

S.J. MARSH

SFA, Inc.,
Landover, Maryland 20785

AND

L.K. LEN AND T. SMITH

FM Technologies, Inc.,
10529-B Barddock Road
Fairfax, Virginia 22032

DTIC
ELECTE
DEC 02 1992
S A D

November 27, 1992

92-30660

REPORT DOCUMENTATION PAGE

Form Approved
OMB No. 0704-0188

1. AGENCY USE ONLY (Leave Blank)	2. REPORT DATE November 27, 1992	3. REPORT TYPE AND DATES COVERED Interim	
4. TITLE AND SUBTITLE Identification of Toroidal Field Errors in a Modified Betatron Accelerator			**5. FUNDING NUMBERS** PE - 47-1485-0-2
6. AUTHOR(S) P. Loschialpo, C.A. Kapetanakos, S.J. Marsh, L.K. Len and T. Smith			
7. PERFORMING ORGANIZATION NAME(S) and ADDRESS(ES) Naval Research Laboratory Washington, DC 20375-5320			**8. PERFORMING ORGANIZATION REPORT NUMBER** NRL/MR/4795—92-7141
9. SPONSORING/MONITORING AGENCY NAME(S) AND ADDRESS(ES) Office of Naval Research, Arlington VA 22217-5000 SPAWAR, Washington, DC 20375-5320			**10. SPONSORING/MONITORING AGENCY REPORT NUMBER**

11. SUPPLEMENTARY NOTES
*Supported by ONR and SPAWAR.
SFA, Inc., FM Technologies, Plasma Physics Div., NRL

12a. DISTRIBUTION/AVAILABILITY STATEMENT Approved for public release; distribution unlimited.	12b. DISTRIBUTION CODE

13. ABSTRACT (Maximum 200 words)

A newly developed probe has been used to detect errors in the toroidal magnetic field of the NRL modified betatron accelerator. Measurements indicate that the radial field components (errors) are 0.1 to 1% of the applied toroidal field. Such errors, in the typically 5 kG toroidal field, can excite resonances which drive the beam to the wall. Two sources of detected field errors are discussed. The first is due to the discrete nature of the twelve single turn coils which generate the toroidal field. Measurements and computer calculations indicate that it's amplitude varies from 0 to 0.2% as a function of radius. This error is a good suspect for causing the excitation of the damaging $\ell = 12$ resonance seen in our experiments. The other source of field error is due to the current feed gaps in the vertical magnetic field coils. A magnetic field is induced inside the vertical field coils' conductor in the opposite direction of the applied toroidal field. Fringe fields at the gaps lead to additional field errors which have been measured as large as 1.0%.

14. SUBJECT TERMS Field Errors Measurements			15. NUMBER OF PAGES 27
			16. PRICE CODE
17. SECURITY CLASSIFICATION OF REPORT UNCLASSIFIED	18. SECURITY CLASSIFICATION OF THIS PAGE UNCLASSIFIED	19. SECURITY CLASSIFICATION OF ABSTRACT UNCLASSIFIED	20. LIMITATION OF ABSTRACT UL

CONTENTS

IDENTIFICATION OF TOROIDAL FIELD ERRORS
IN A MODIFIED BETATRON ACCELERATOR

I. INTRODUCTION

The NRL modified betatron is a compact (1 m major radius) cyclic device that has achieved energies in excess of 20 MeV, while the trapped current is in excess of 1 kA. This device has been described in previous papers. [1-4] During the beam acceleration phase three independently controlled magnetic fields are externally applied to the beam. A vertical magnetic field rises sinusoidally in time from 0 G to typically 1200 G peak amplitude in 2.6 ms. The vertical field serves to inductively accelerate the beam and confine its orbit about the major axis. A toroidal magnetic field, B_θ, is also applied which sinusoidally rises to a typical peak amplitude of 5 kG in 2.28 ms. This toroidal field is needed to confine the minor radius of the high current beam. A strong focusing magnetic field was also found necessary to trap the beam and help with stability during acceleration. [2] This field is produced by stellerator windings which are four twisted windings that carry current in opposite directions. The windings which are located 23.4 cm from the minor axis can carry a peak current of 32 kA.

The beam lifetime in the NRL modified betatron is limited by the cyclotron resonances. The theory describing these resonances has been previously developed. [5,6] In simple terms, whenever the number of poloidal revolutions about the toroidal field for each orbit about the major axis is an integer a stationary field error can excite a resonance. With considerable effort several field errors have been detected and reduced in the experiment.[3] An increase in the obtainable beam energy from 12 MeV to 18 MeV has resulted from this effort.

This paper reports efforts to measure some of the remaining field errors, particularly

those which are associated with the applied toroidal magnetic field. The toroidal field is generated by twelve discrete rectangular coils. Four legs form this rectangle which is located on a plane of constant toroidal angle, θ. Each toroidal field coil leg is constructed from a square cross section aluminum tube with an outside dimension of 10.2 cm and a wall thickness of 1.3 cm. A schematic of the toroidal field coils and the associated field, B_θ, is shown in Fig. 1. This figure also illustrates one type of field error associated with the toroidal field, namely a ripple with a 30° toroidal period which is due to the discreteness of the coils. The radial component of this ripple is measured with a probe that has toroidally curved windings facing the radial direction. The coil is counterwound to reinforce the probe output signal produced by the oscillating B_r. A probe which has eleven such coils to measure B_r as a function of the major radius, r, is described in detail in part II. Techniques used in making these measurements are described. Experimental results are presented in part III and are compared with numerical computations. In addition to the field error just mentioned another source of field error has been discovered by this probe. This will be discussed in detail later, but briefly it arises from gaps in the vertical field coil loops. At these gaps a transition is made to a coaxial geometry in order to feed current to the vertical field coils. The effect these field errors may have on beam stability is discussed.

II. APPROACH TO MEASUREMENT OF TOROIDAL FIELD ERRORS

A. Design of the probe

The design goal of the toroidal field error probe was the capability of measuring a radial magnetic field of less than 1 G in a background toroidal field of 1000 G. In addition, the probe should provide the radial profile of toroidal field errors in one shot to speed up

data collection and ease concerns about reproducibility. The primary time span of interest was the first 2500 μs after the initiation of the toroidal field.

Each of the eleven probe channels which measure B_r at a particular major radius, r, consists of a pair of coils. The loop area of each coil senses the time derivitive of the radial field, dB_r/dt, integrated over the area of the coil. A high density polyethylene spool serves as a coil form. Each of the 22 required coil forms has a rectangular cross sectional area with vertical and toroidal dimensions at the coil groove bottom of 1.52 cm and 21.11 cm, respectively. The groove in each coil form is 0.32 cm wide, 0.38 cm deep on the top and bottom, and 0.64 cm deep on the ends. A coil form is wound with six layers of 25 AWG copper magnet wire which has been measured to be 0.051 cm diameter with the insulation included. Each layer is six turns wide and has a light coating of a fast drying polystyrene resin which held the individual turns together during the winding process. The total number of turns for each coils is therefore N=36. Great care was taken to insure that for every layer each turn has been laid flat next to the preceeding turn. No wires were allowed to cross over one another. After winding the coil any remaining space was filled with RTV615 silicone rubber potting compound.

The 22 coils were individually calibrated to determine their response to a known magnetic field which is uniform over the coil area. The passively integrated signal output from a single coil is given by $V=NAB_r/RC$ for $t<<RC$. Here A is the effective cross sectional area of the coil, B_r is the applied field, and RC =1.87 ms is the measured integrator time constant for the calibration. The calibration field was produced by a 45 turn pair of 61.6 cm diameter coils, spaced 32.0 cm apart (center to center), arranged in

3

a solenoidal configuration. Calculations with the EFFI[7] computer program indicate that the axial field was 1.28 G per ampere drive current at the center of the effective solenoid and drooped off about 1% at the ends of the coil form. The calibration drive current, produced by a capacitive discharge into an overdamped L-R-C circuit, was monitored with a Pearson current monitor simultaneously with the passively integrated probe coil response. Measurements were taken 60 μs after the initiation of the recorded waveforms. A typical drive current was 3.6A. The result of this calibration procedure is a known value of NA for each coil which ranges from 0.142 m^2 to 0.148 m^2, which has a 4.1% spread. Self inductance for a probe coil was measured to be 570 μH.

Following calibration, the coils were inserted into matching machined grooves of a phenolic coil mount. The eleven pairs of coil grooves, shown in Figs. 2 (a-b), are machined to a radius of curvature equal to the major radius at which the coils were positioned when the probe was mounted on the modified betatron. Each pair of coil grooves with the same radius of curvature is separated by a narrow partition (0.14° arc length) on the toroidal symmetry plane of the coil mount which has a 30° arc length. Coils on the connector panel side are wound in the opposite direction of coils on the other side of the toroidal symmetry plane. When the probe's toroidal symmetry plane is aligned with a toroidal field coil, as in Fig. 1, and for the case where no field errors other than the toroidal field coil discreteness is present then the signals picked up by each half of the probe reinforce. The expected output signal polarity of the probe is negative for the direction of B_r shown in Fig. 1. Because of the toroidal symmetry, moving the probe 15° to align the toroidal symmetry plane between two toroidal field coils would result in a positive polarity signal with the same amplitude. The eleven coil pairs are mounted 1.5 cm apart on center starting with

4

r = 90.0 cm (channel 1) and ending with r=105.0 cm (channel 11) and during operation are centered on the midplane of the modified betatron.

In order to measure B_r in the presence of $B_\theta > 1000 \, B_r$ the net loop area facing the θ direction must be substantially less than $2NA/1000 \approx 3 \text{ cm}^2$. This was the motivation for machining the coil grooves with a radius matching the modified betatron major radius. As each coil was bent to be inserted into a groove, care was taken to avoid wire slippage which might cause a B_θ pickup. The windings appeared to follow the toroidal curvature well. In making connections between coil pairs and from coils to connectors all stray loop areas were minimized and any remaining loop area was oriented to face the radial direction.

Another advantage of counterwound coil pairs for each channel is that the probe output is insensitive to small rotational errors about an axis perpendicular to the midplane. Signal pickups on either side of the probe's toroidal symmetry plane cancel to first order, provided that each coil pair has the same NA. This is very nearly the case since coils with the closest calibrated values of NA were paired opposite one another. The worst case is for channel 10 for which the values of NA differ by approximately 1% of the combined area of 0.293 m^2 for that channel. It should be noted that since the length of each coil is the same they span different arc lengths depending on the curvature radius, r_c, of the groove in which it sits. Including a correction for the thickness of the windings, the effective coil length is L = 21.5 cm. The arc length which a coil spans is given by $\Delta\theta=180 \, L/\pi \, r_c$ which is 13.7° for channel 1 and 11.7° for channel 11.

B. Measurement technique

The probe was installed on the modified betatron in order to measure only radial

5

components of magnetic fields. Looking downward, the toroidal coordinate of the probe symmetry plane is measured counterclockwise from the electron beam injector which is located midway between two toroidal field coils. The elevation of the probe was set to align the vertical symmetry plane of its coils with the midplane of the accelerator.

Signals from the eleven coils were run through electrically isolated coaxial cables into a shielded room. These signals were terminated with 50 Ω resistors, passively integrated, and fed to individual input channels among three Lecroy 6810 digitizers. After each shot, recorded waveforms were stored on a computer for later processing. The RC time constant of each of eleven integrators was measured and found to range from 18.8 ms to 20.4 ms. An integrator was permanently assigned to each probe channel. From the equation V=NA$< B_r >$/RC, where $< B_r >$ is the radial field averaged over the length of a coil pair, and from the calibrated values of NA the signal response of each probe channel was determined. The values of $< B_r >$/V ranged from 0.66 G/mV to 0.70 G/mV. Vertical resolution of the digitizer is 0.1 mV on the most sensitive setting which corresponds to 0.07 G. Processing the waveforms consisted of numerically filtering out high frequency noise, subtracting any baseline offset and vertical scaling to yield values of $< B_r >$ as a function of time.

As was previously mentioned, radial positioning of the probe is important so that the curvature of the pickup coils matches the curvature of the toroidal field lines. This was determined experimentally by measuring with a scale the distance from the outer edge of the probe to the machined cylindrical surface of a spline which is permanently stationed on the center of the modified betatron. Combined uncertainties in this measurement are

6

estimated to be ± 0.1 cm. The stray B_θ pickup from a radial displacement error, d, can be estimated. Let θ_c be the arc length spanned by a coil with radius of curvature r_c and height h. The coil area facing the toroidal direction due to this radial displacement for a given channel is

$$A_\theta = 2Nh[d + r_c(1 - \sqrt{1 + (\frac{d}{r_c})^2 + 2\frac{d}{r_c}cos\theta_c})]. \tag{1}$$

A factor of two appears just to the right of the equal sign because the signal picked up by the two coils of a given channel add together. For small positioning errors $d \ll r_c$ and Eq. 1 reduces to

$$A_\theta = 2Nhd(1 - cos\theta_c).$$

A good estimate of the coil height, including a correction for the coil winding thickness is h=1.9 cm. The error is worst for the innermost coil pair for which θ_c=13.7°. In this case, with d=0.1 cm, the coil area facing the toroidal direction is A_θ = 0.39 cm^2. The stray pickup appears as an erroneous field. The ratio of this erroneous field to B_θ is B_r, $_{err}/B_\theta$ = A_θ/2NA = 1.3 x10^{-4} which is reasonably small.

Vertical positioning of the probe on the midplane was determined with a survey transit to ± 0.05 cm. Experience with the probe has demonstrated that small displacements such as this are negligable. The toroidal positioning was done with respect to the center of the toroidal field coils. This measurement was made with a precision of ± 0.15 cm and variations in position of this magnitude appeared to have a negligable effect on the probe's output. The toroidal position of the inner toroidal coil vertical legs is fixed to a high

7

accuracy by the machined spline at the betatron's center. However, the outer vertical legs had a positional uncertainty of ±1.5 cm. It turns out this has a significant effect on B_r which will be discussed in subsequent sections.

Care was taken to avoid rotation of the probe around an axis perpendicular to the midplane within a tolerance of ± 0.1 cm. Analysis and experiments show that there is no significant stray pickup for rotational errors of this magnitude.

III. RESULTS

A. Errors due to toroidal field discreteness

As stated in the introduction and is illustrated in Fig. 1, the discreteness of the toroidal field coils produces a radial field component. This induces a ripple in the toroidal field lines with a 30° period in θ. Figure 3 shows the toroidal field at r=100 cm, measured with a calibrated field coil. It should be noted that this is roughly one half of the actual operating field in order to reduce physical demands on the driving circuit.

In Fig. 4 waveforms are presented showing $< B_r >$ with the probe centered at θ=330° (between two toroidal field coils). Because of the 30° periodicity of these coils this situation is similar to that of Fig. 1 with the probe centered about one coil except for a change of sign in the measured signal. These waveforms have the same shape as the applied B_θ waveform. At r=90.0 cm the signal has a positive polarity which means, from the known winding direction of the coils, that the toroidal field lines are bulging inward toward the major axis. In other words, at the upstream side of the probe (that side with the smaller toroidal angular position) $B_r < 0$ and at the downstream side $B_r > 0$. Except for a small stray pickup associated with each coil, the trend of the waveforms indicates that $< B_r >$

8

changes polarity and then continues monotonically increasing with radial distance. We refer to the radius at which $B_r = 0$ as the "toroidal field axis". It can be seen that the toroidal field axis is substantially inward from the minor axis of the device.

The solid circles in Fig. 5 show the radial field at t = 2280 μs (measured from the initiation of the waveform) as a function of r. Data are from the waveforms of Fig. 4. The values have all been divided by 2.27 kG, which is the measured value of B_θ at t=2280 μs and r=100.0 cm. In addition, each of the measured radial field amplitudes have been multiplied by a scaling factor ranging from 0.924 for r=90.0 cm to 0.862 for r=105.0 cm. This scaling operation yields $< B_r >_{30}$ which is the radial field averaged over a 30° toroidal sector rather than the radial field averaged over a counterwound coil pair. The scaling assumes that the toroidal dependence of B_r is sinusoidal with a period of 30°. Calculations have shown this assumption to be valid to a high degree of accuracy. In Fig. 5 (a) the solid curve represents the calculated value of the same field. The calculations were done using a computer program which solves the Biot-Savart law for coils composed of single filaments. Four filaments are connected to form a rectangular toroidal field coil loop. Two horizontal filaments lie 69.7 cm above and below the midplane. These are joined by two filaments at r=45.7 cm and at r=169.9 cm. All four filaments lie on a plane of constant θ. Two such filament loops with the same current are on either side of the probe, one at $\theta = 315°$ and the other at $\theta = 345°$. Physically, these filament loops lie on the center of the inner surface of the actual toroidal field coils. We presently have no way of measuring the actual current distribution in the toroidal coils cross section. However, current flowing preferentially on the inner surface minimizes the circuit inductance so it is physically reasonable to assume that this is approximately the case. The caption "θ offset = 0.00 cm" refers to both

9

toroidal current loops being perfectly alligned 30° apart. Experimental data indicates the toroidal field axis is near r=92 ± 2 cm and that $< B_r >_{30} /B_\theta$ is approximately -0.15% at the minor axis. Calculations show the toroidal field axis to be at r=86.5 cm and that $< B_r >_{30}/B_\theta$ =0.205 % at the minor axis. The fit of the calculated values of $< B_r >_{30}$ to the data is substantially improved if the outer vertical leg of one of the toroidal filament loops, at r=169.9 cm, is moved closer to the other by 0.50 cm. This case is shown in Fig. 5(b). The same data plotted in Fig. 5(a) are plotted in Fig. 5(b) for convenience in making comparisons. In this case, calculations indicate that the location of the toroidal field axis is at r=89.5 cm, while the value of $< B_r >_{30}/B_\theta$ at the minor axis is -0.165% for a -0.50 cm θ offset. Following these calculations, a careful survey was made of the toroidal field coils. The outer legs of the coils at $\theta = 315°$ and $\theta = 345°$ were found to be toroidally displaced 0.5 cm and 1.0 cm, respectively. Consequently, the gap spacing for these toroidal field coils is 0.5 ± 0.2 cm too small. Computer calculations indicate that the toroidal field distribution , $B_r(\theta)$, is sensitive to which of the two outer coil legs is displaced. However, the average field, $< B_r >_{30}$, only depends on the gap spacing of the outer coil legs. Therefore, the radial field measured by the probe appears accurate within the tolerance of the measured toroidal field coil. In making this survey in was found that, for some of the coils, the separation between adjacent vertical legs exceeded the proper distance by as much as 1.5 cm. Further calculations show this results in an inward shift of the toroidal field axis to r=81 cm and at the minor axis $< Br >_{30} /B_\theta$ becomes -0.33%. Preliminary computer simulations indicate that the detrimental effect of this misalignment on beam stability is quite significant.

B. Errors due to feeds of the vertical field coils

10

During the measurements another field error source was unexpectedly encountered. This source arises from gaps in the vertical field coil loops which are necessitated by coaxial current feeds to these coils. Except for the gaps the vertical field coils are geometrically circular loops which are coaxial with the major axis and lie in a plane parallel to the midplane of the device. They are situated in pairs at equal distance above and below the midplane. The conductor is a hollow aluminum tube with a square cross section measuring 7.6 cm on a side and having a 0.63 cm wall thickness. Even though the vertical field coils are not energized the applied B_θ induces a toroidal field inside the vertical field coils which opposes the applied field. For times much less than the magnetic field diffusion time, the induced toroidal field is comparable in magnitude with the applied B_θ. In the presence of a gap the induced field lines will diverge, producing a negative B_r component on the upstream side of the gap and a positive B_r component on the downstream side for positions radially outside of the gap. This situation is illustrated schematically in Fig. 6.

Due to its proximity to the region of interest, it is expected that the gap of the vertical field coil pair nearest the midplane, labelled VF± 1, would produce one of the largest field errors of this type. The radial and vertical positions (measured from the midplane) for VF±1 are r=70.75 cm and z=± 7.5 cm. Since the toroidal position of the center of the gaps for the VF ± 1 coils is at $\theta = 60$ °, midway between two toroidal field coils, the induced B_r components are in the opposite direction to the B_r components that are due to the toroidal field coil discreteness. This field error was measured with the probe centered at $\theta = 60°$. The results, plotted in Fig. 7, show the total radial field, averaged over the length of a coil pair, as a function of major radius for three times following initiation of the pulse. For each of these three times the averaged radial field has been divided by the applied toroidal

11

field at that time given in Fig. 3. At r=90 cm, the field error is $< B_r > /B_\theta \approx 0.8\ \%$. This is much larger than the measured field error caused by the coil discreteness. The rapid decline of $< B_r > /B_\theta$ with increasing r is qualitatively consistant with a localized dipole field error at the VF $\pm$ 1 coil gap. Because $< B_r > /B_\theta > 0$ the induced B_r component dominates the B_r component of the applied toroidal field ripple. Locally, this results in a net inward bulge to the total toroidal field lines and a toroidal field axis which is driven outward to r=105 cm. Figure 7 also shows that $< B_r > /B_\theta$ is practically independent of time for t< 2.28 ms. This implies that the characteristic magnetic diffusion time for this geometry are much longer than 2.28 ms. A rough calculation of the diffusion time into the VF $\pm$ 1 coil, using $\tau = \frac{\mu_o\ r_{eq}\Delta}{2\rho}$, yeilds $\tau \approx 6$ ms.[8] In the above equation μ_o is the permeability of free space, r_{eq} is the equivalent radius of a circle having the same area as the vertical field coil cross section, $\Delta = 0.63$ cm is the coil wall thickness, and ρ=2.65 x 10 $^{-6}\Omega - cm$ is the elctrical resistivity of aluminum. This diffusion time is not very much larger than 2.28 ms. At this time, we do not fully understand why $< B_r > /B_\theta$ is independent of time. It may be due to the construction of the coil connection which is solid aluminum except for the part at the transition to the coaxial feed. A complete quantitative understanding would require three dimensional, time dependent simulations which we have not done at this time.

To further investigate this field error the probe was centered at $\theta = 330°$ again, where the data of Figs. 4 and 5 were taken. The coaxial feed (risers) and coil connection were removed from the VF $\pm$ 1 coils and the gaps were rotated to be centered at θ =330°. Results from these measurements are plotted in Fig. 8. Notice that in this case the field error decreases significantly with time, dropping from 0.97% to 0.73% at r=90 cm.

Magnetic flux can diffuse appreciably into the thin VF± 1 coil walls in this time frame. Since this type of local field error is expected to decrease rapidly with distance it is also reasonable that the toroidal field axis, r=105 cm in this case, is the same as in Fig. 7. One feature about the data in Fig. 8 is quite surprising. With the removal of the coaxial feed and coil connection shown in Fig. 6, the gap width should be much larger than before. Yet the increase in field error is only slight. This feature is not yet understood.

Field errors of this magnitude can create significant transverse forces on the beam. In order to evaluate the effect of such a field error on beam dynamics the feeds for the VF ± 1 coils have subsequently been rotated from θ=60° to $\theta = 270$°. Preliminary comparisons of the toroidal distribution of beam loss before and after this change indicate a substantial new beam loss peak near θ=270°. It should be mentioned, however, that these toroidal beam loss distributions are not yet fully understood and are being investigated.

IV. CONCLUSIONS

We have developed a magnetic field probe which has the ability of resolving time dependent radial field components (errors) in an applied toroidal field which are as small as 0.05% of the main field component. Experimental data compared well with computer calculations for the case where no vertical field coil gaps are present. In this case, the measured radial field error is approximately -0.15% and the calculated value is -0.165% at the minor axis (r=104.5 cm). This field error is due the toroidal field coil discreteness. It is increased in amplitude by -0.04% to -0.205% when the misaligned toroidal field coil is moved by 0.5 cm, opening the gap between toroidal field coils, to the correct position.

With this probe a second source of field errors has been identified. This arises from

13

the divergence of the induced flux at the gaps, where current is fed. For the gap in the VF $\pm$ 1 coil pair the measured error is quite large and independent of time for the period of interest. At r=90 cm the average radial field error is 0.8%. For the case when the coaxial feed and coil connection are removed from the vertical field coil this error rises only slightly to 0.97% at t=1000 μs. At t=2280μs this field error decreases to 0.73%. This field error source exists at four other locations around the modified betatron.

Further experiments have begun in an attempt to assess the importance of these field errors. Rotation of the VF$\pm$ 1 coil gaps from $\theta = 60°$ to θ=270° has resulted in a considerable change in the toroidal distribution of beam loss with a new peak occuring near $\theta = 270°$.

ACKNOWLEDGEMENTS

References

1. L.K. Len, T. Smith, J. Golden, K. Smith, S.J. Marsh, D. Dialetis, J. Mathew, P. Loschialpo, J.H. Chang, and C.A. Kapetanakos, *Proceedings of International Society for Optical Engineers (SPIE)* (SPIE, Bellingham, WA, 1990), Vol. 1226, p. 382.

2. C.A. Kapetanakos, L.K. Len, T. Smith, J. Golden, K. Smith, S.J. Marsh, D. Dialetis, J. Mathew, P. Loschialpo, and J.H. Chang, *Phys. Rev. Lett.* **64**, 2374 (1990).

3. J. Golden, L.K. Len, T.J. Smith, D. Dialetis, S.J. Marsh, K. Smith, J. Mathew, P. Loschialpo, L. Seto, J.H. Chang, and C.A. Kapetanakos, *Proceedings of International Society for Optical Engineers (SPIE)* (SPIE, Bellingham, WA, 1991), Vol. 1407, p. 418.

4. C.A. Kapetanakos, L.K. Len, T. Smith, D. Dialetis, S.J. Marsh, P. Loschialpo, J. Golden, J. Mathew, and J.H. Chang, *Phys. Fluids B* **3**, 2396 (1991).

5. D. Chernin and P. Sprangle, *Part. Accel.* **12**, 101 (1982).

6. C.W. Roberson, A. Mondelli, and D. Chernin, *Part. Accel.* **17**, 79 (1985).

7. S.J. Sackett, *Report UCRL*-52402, Lawrence Livermore Nat'l. Lab., Livermore, CA (1978).

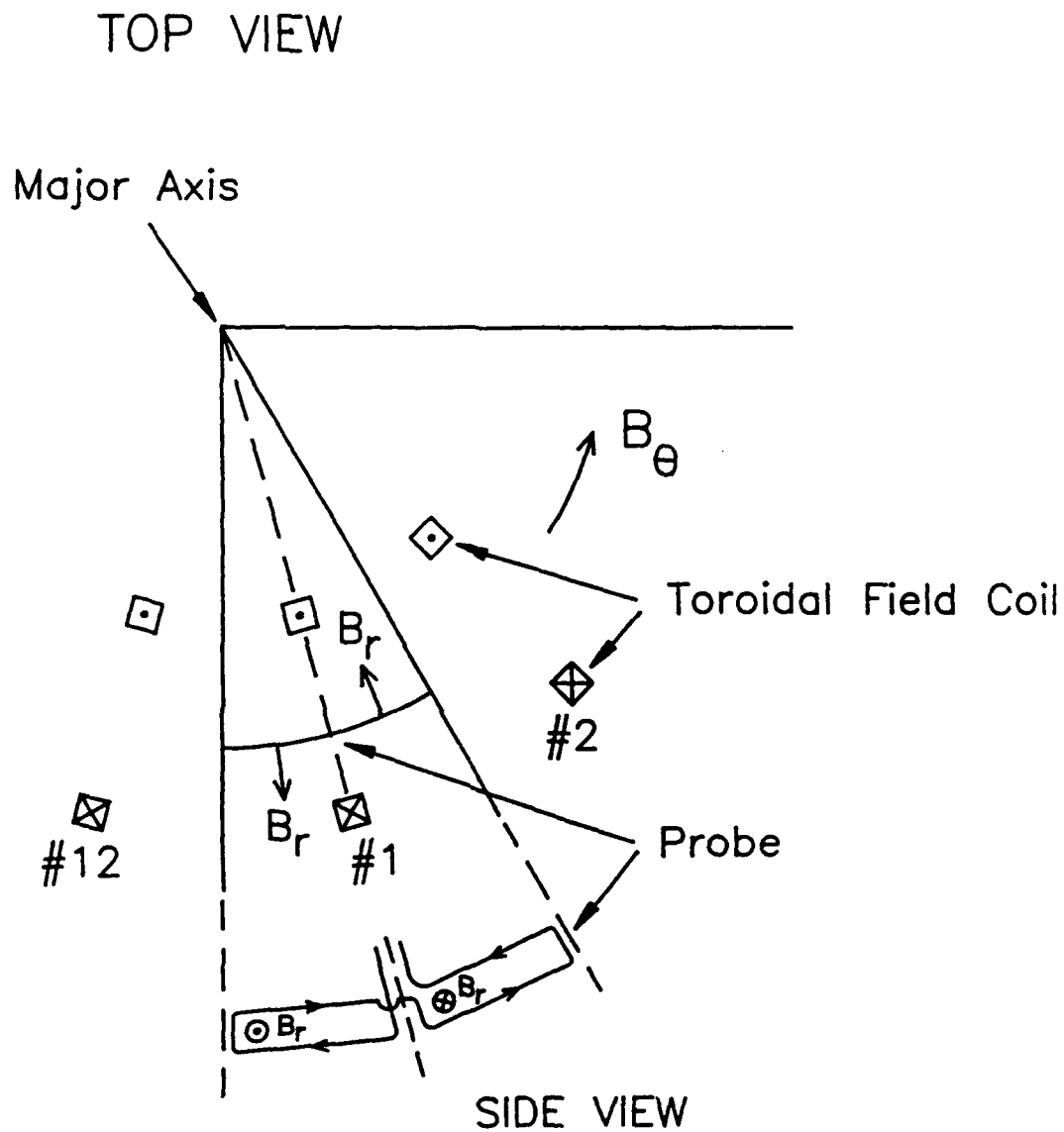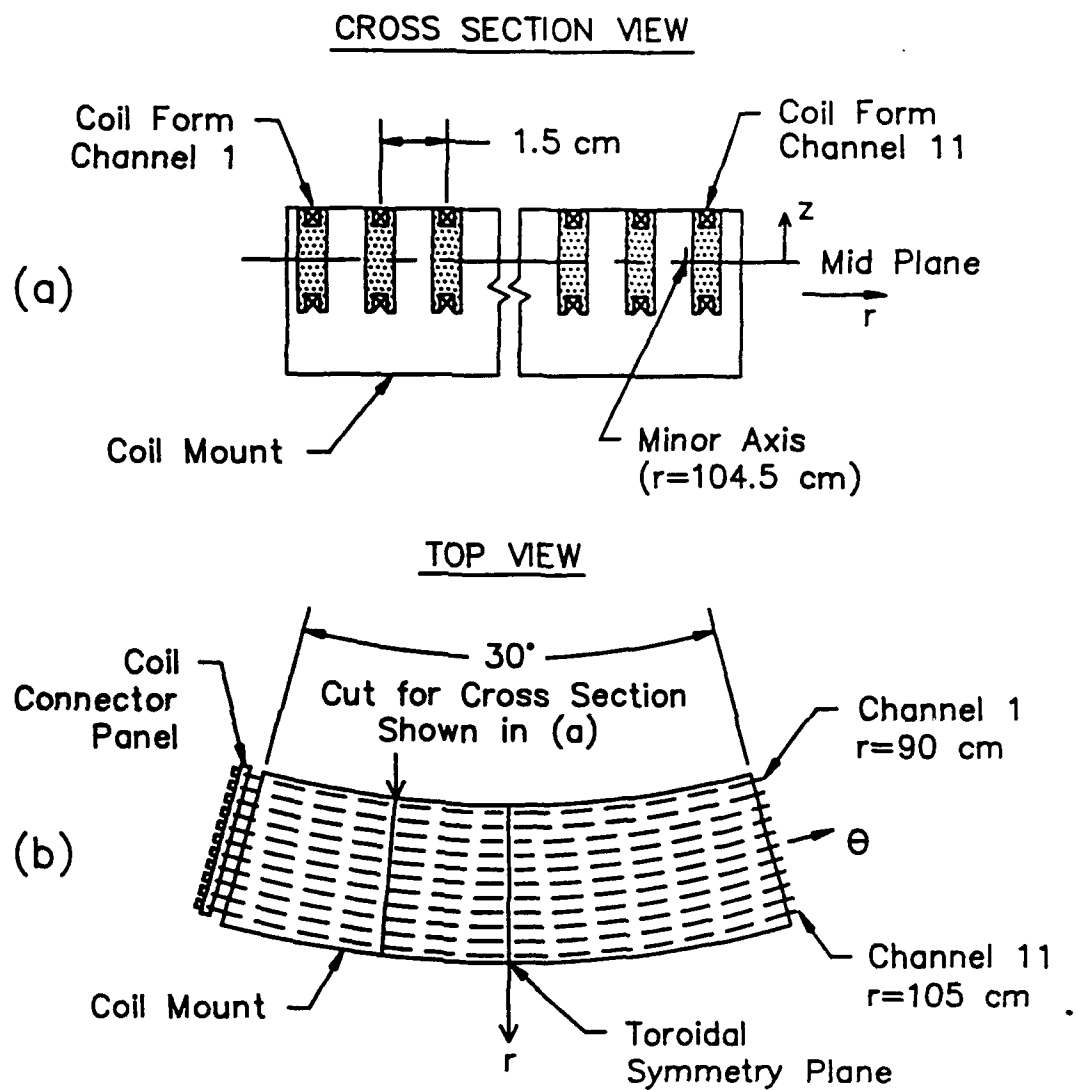8. Heinz Knoepfel, *Pulsed High Magnetic Fields* (American Elsevier, New York, 1970), p. 97.

Fig. 1. Schematic of toroidal field coils and their associated magnetic field over two 30° sectors. The radial component of this field, B_r, due to the discreteness of these coils and a probe to measure B_r are also schematically illustrated.

CROSS SECTION VIEW

(a)

Coil Form
Channel 1

1.5 cm

Coil Form
Channel 11

z

Mid Plane

r

Coil Mount

Minor Axis
(r=104.5 cm)

TOP VIEW

(b)

Coil
Connector
Panel

30°
Cut for Cross Section
Shown in (a)

Channel 1
r=90 cm

θ

Coil Mount

Toroidal
Symmetry Plane

Channel 11
r=105 cm

r

Fig. 2. Construction of the probe developed to measure B_r. (a) Cross section view of coil

mount which supports 11 wound coil forms and (b) top view of coil mount.
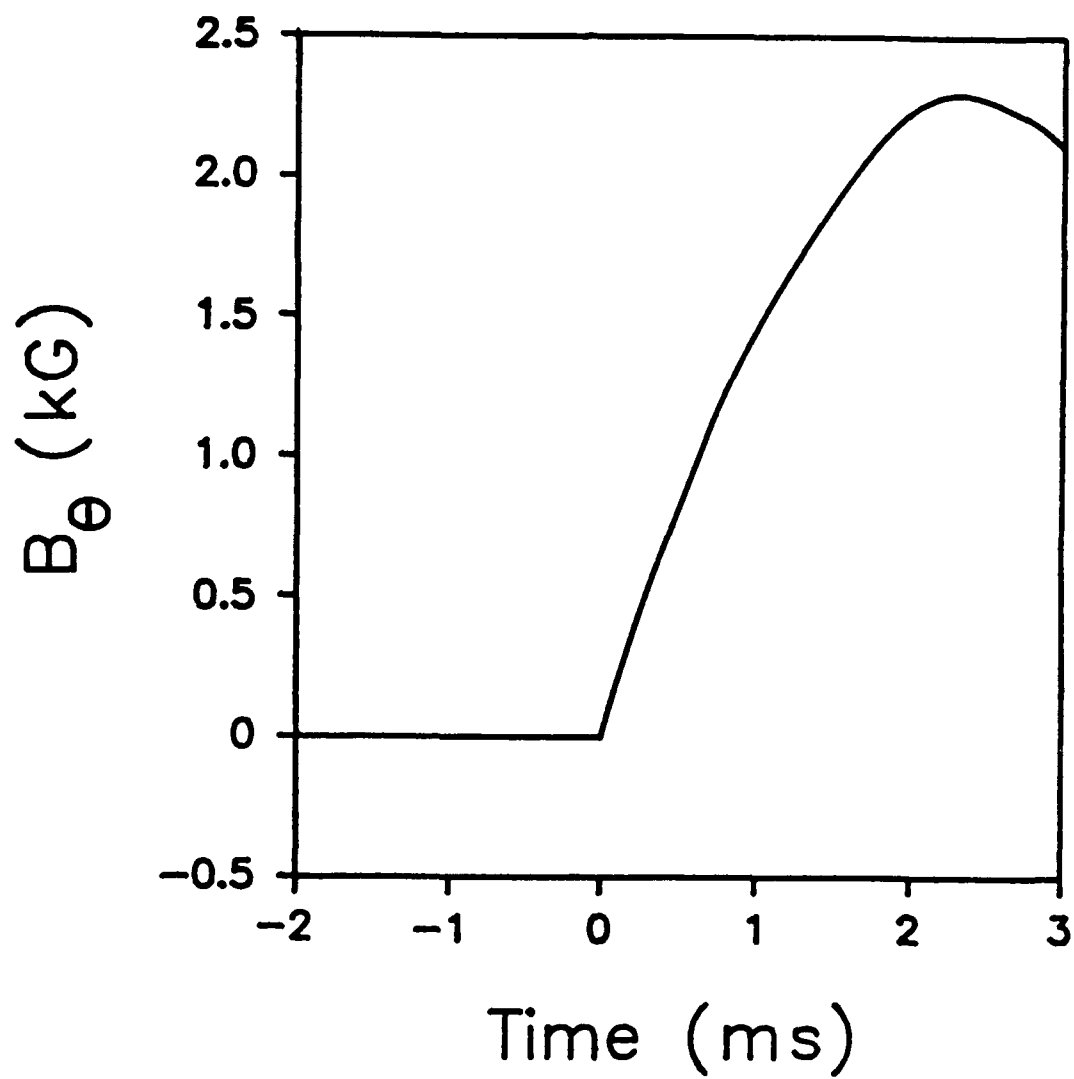
Fig. 3. Applied toroidal field as a function of time at r=100.0 cm for field error measurements.
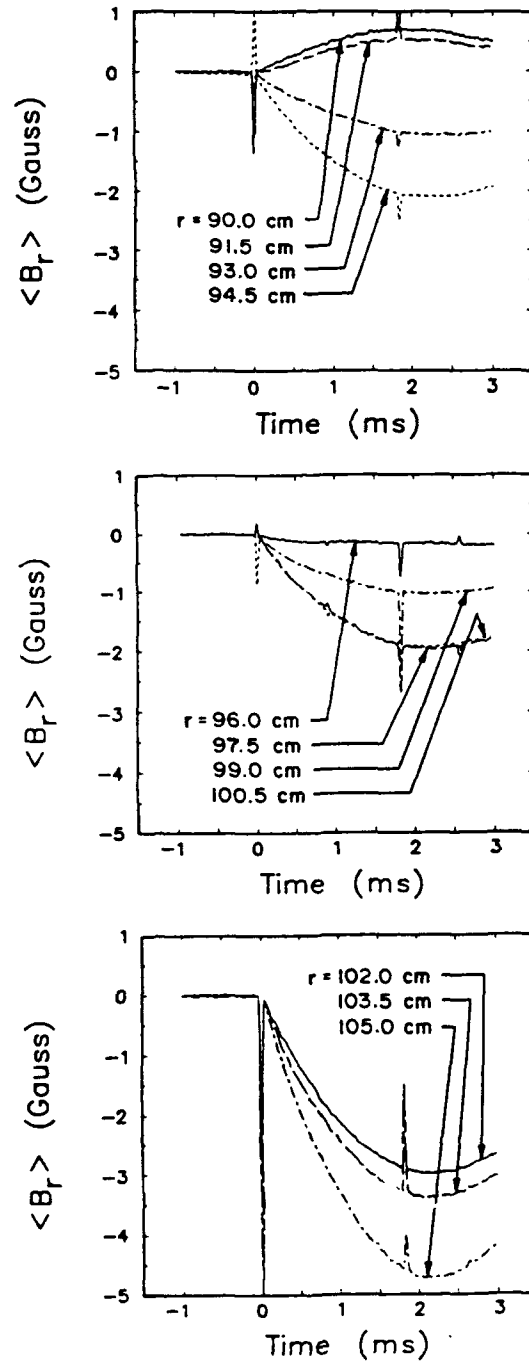
Fig. 4. Radial field averaged over the length of each probe coil pair versus time for each of the probe channels. The toroidal symmetry plane of the probe is at $\theta = 330°$ and no vertical field coil gaps are nearby.
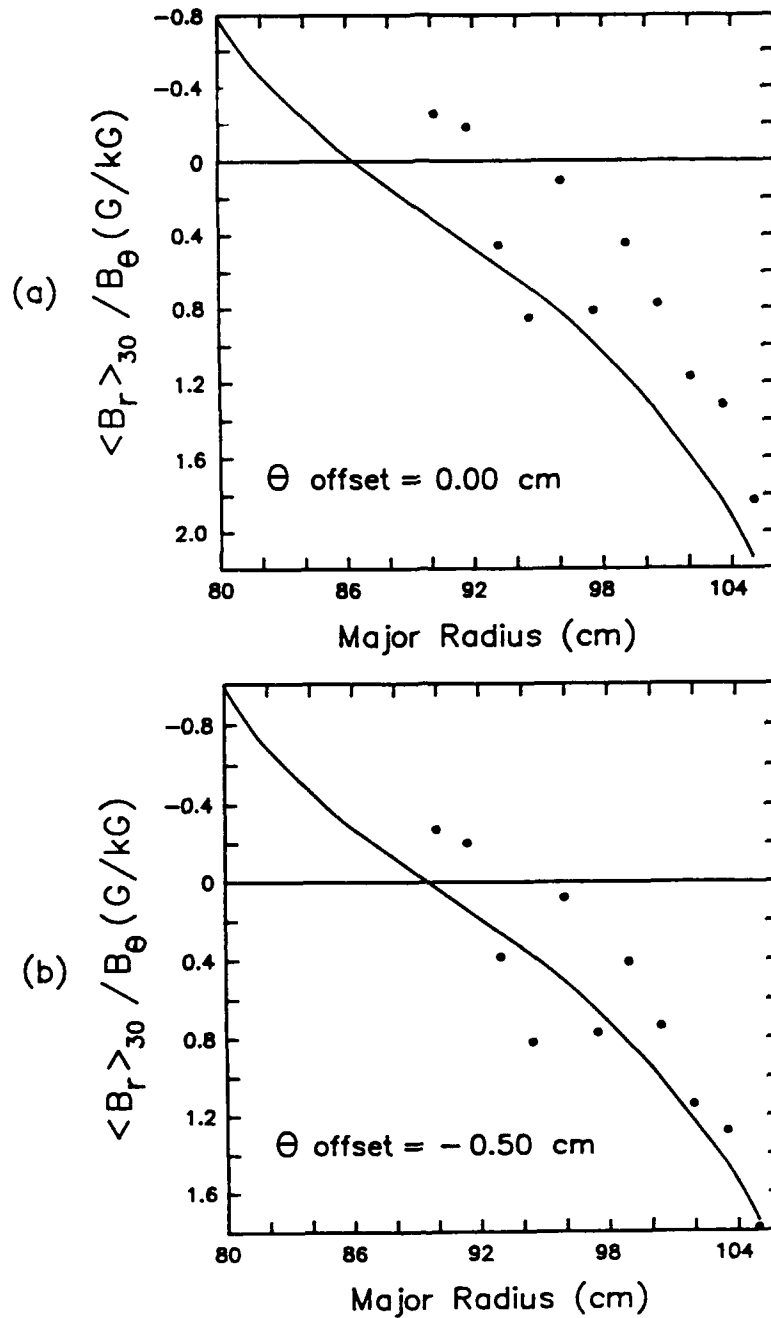
Fig. 5. Radial field averaged over a 30° toroidal arc length and normalized to B_θ at r=100.0 cm, t=2280 μs versus major radius. The toroidal symmetry plane of the probe is $\theta =$ 330° and no vertical field coil gaps are nearby. Solid circles represent measured data and the curve represents computed values from a pair of toroidal coil filaments. (a) Computed values with toroidal coils perfectly positioned, and (b) with outer toroidal coil legs spaced 0.5 cm too closely in the toroidal direction. Data are the same in (a) and (b).
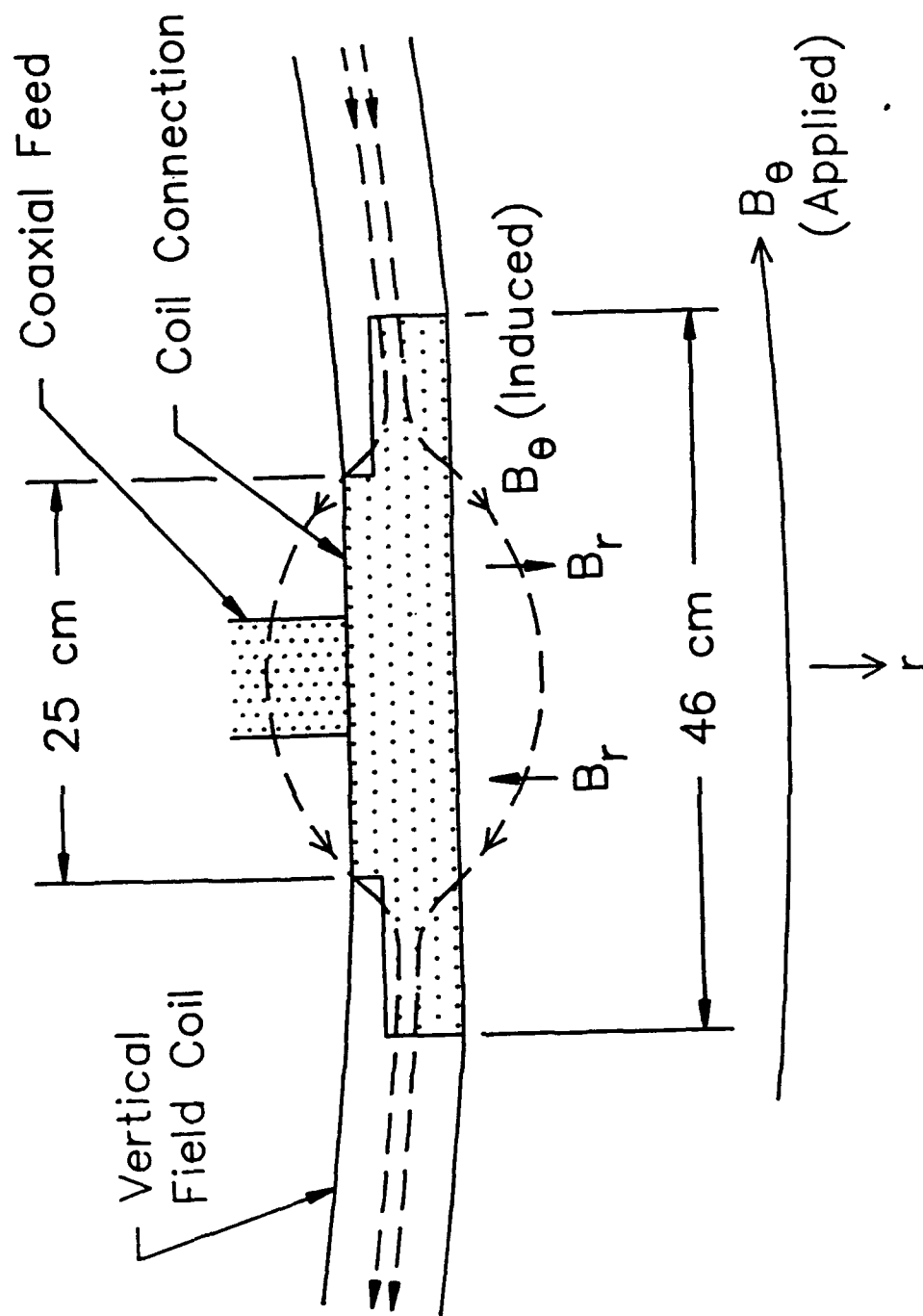
Fig. 6. Schematic illustrating the effect of the coaxial feed to vertical field coil transition on the field generated by the toroidal field coils.
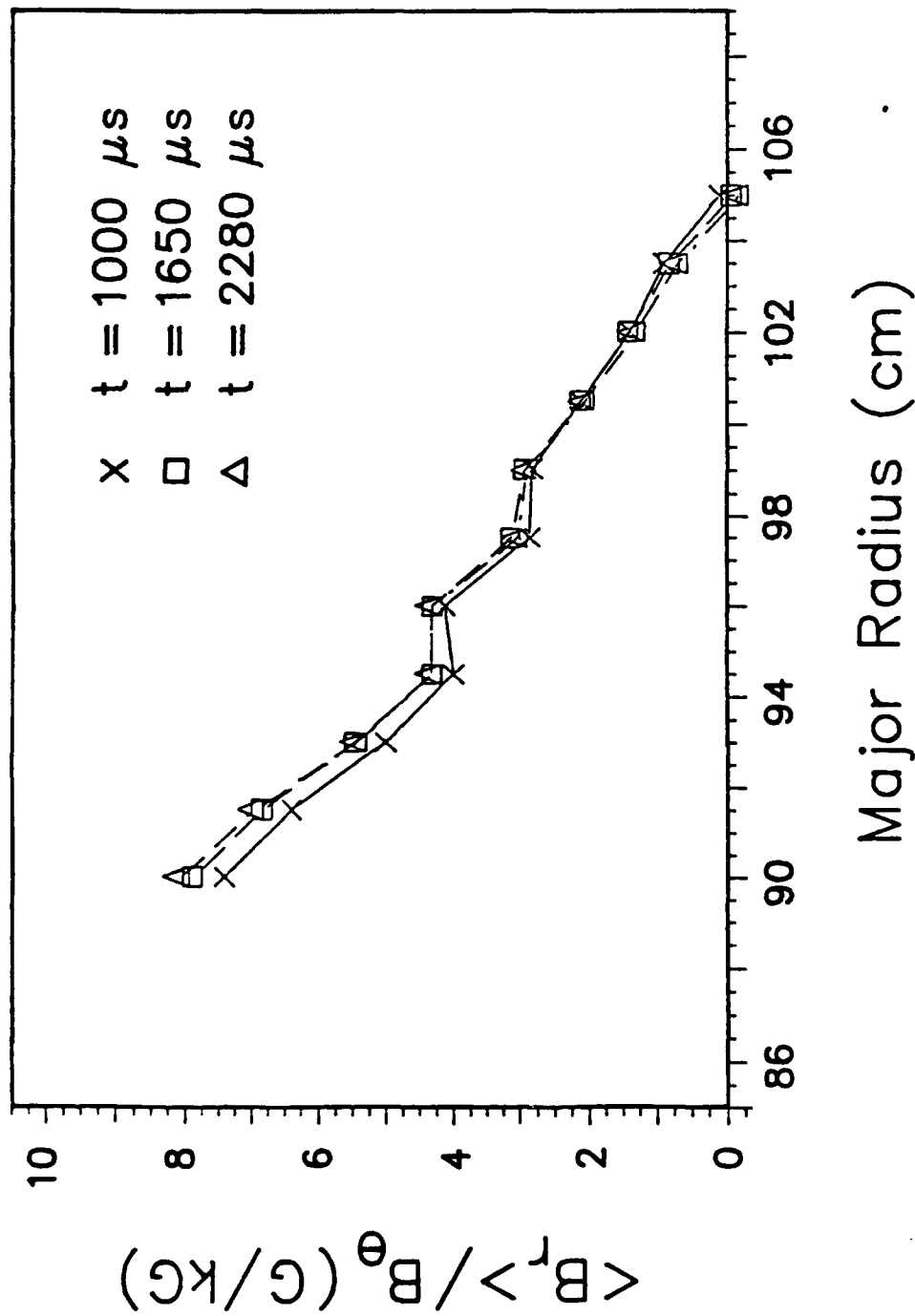
Fig. 7. Experimental values of the radial field averaged over the length of each probe coil pair, normalized to B_θ at r=100.0 cm, versus major radius for the three times shown. The probe's toroidal symmetry plane is at $\theta = 60°$, alligned with the coaxial feed transitions to the VF± 1 coils.
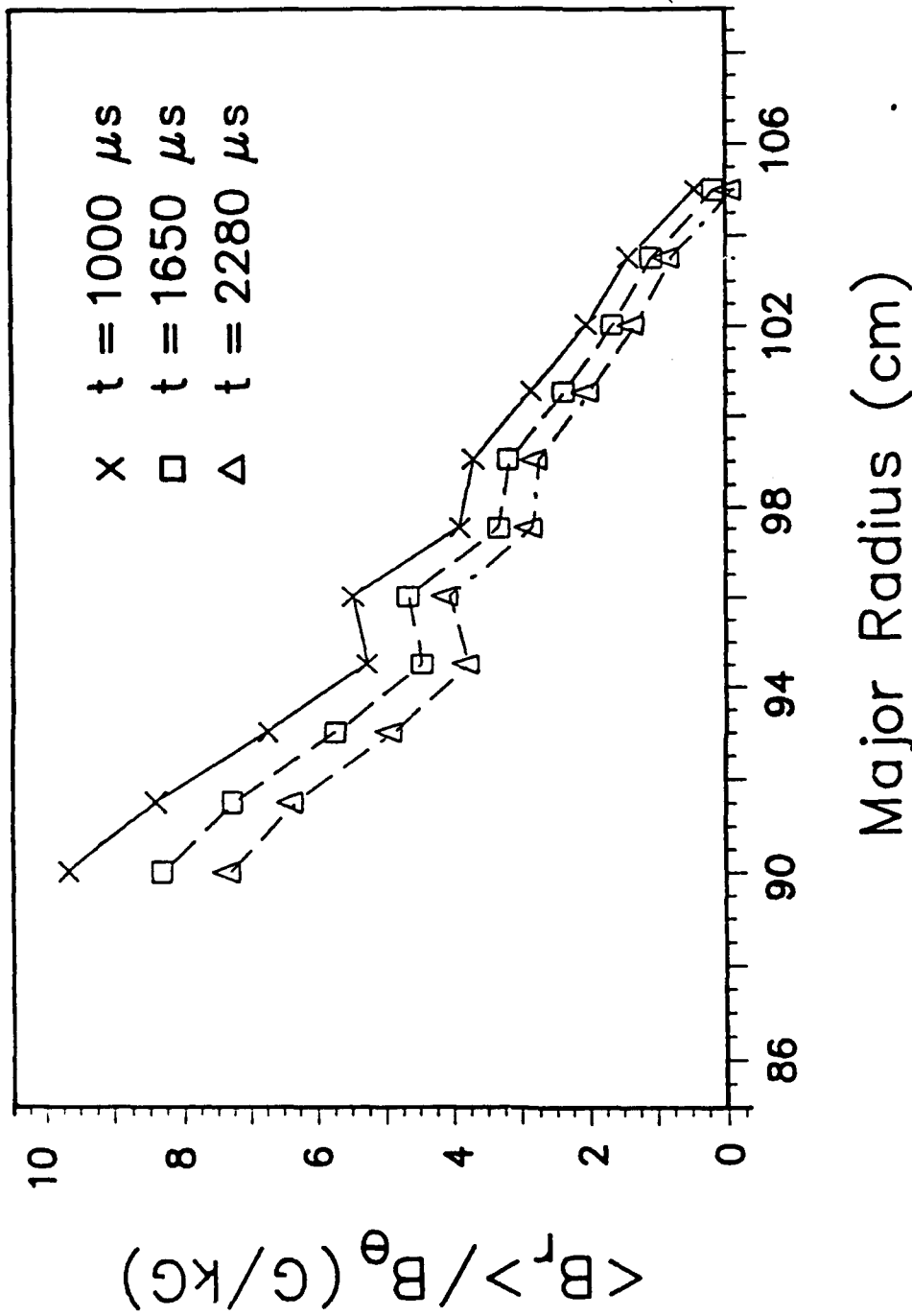
Fig. 8. Experimental values of the radial field averaged over the length of each probe coil pair, normalized to B_θ at r=100.0 cm, versus major radius for the three times shown.

The probe's toroidal symmetry plane is at θ=3.30°, alligned with the gap remaining in the VF±1 coil pairs after the coaxial feed and coil connections have been removed.